It is worthwhile mentioning here that the forms of J_{z1} and $\tilde{J}_{z1}$ are identical to those used by Denlinger [5].

A similar expression can be used for higher order $\tilde{J}_{zi}$ and $\tilde{J}_{xi}$. The dispersion relation has been calculated for two choices of matrix size: 1) $N = 1, M = 0$ and 2) $N = M = 1$. In the first case only the axial component J_{z1} of the step current is retained. This case may be called the zero-order approximation while choice 2) is the first-order approximation.

It should be noted that, although the computation of matrix elements given by (8) involves the evaluation of infinite summations, these summations can be efficiently evaluated, since for large n each term in the summations behaves as $(\hat{k}_n w)^{-3}$.

Fig. 2 shows the effective dielectric constant computed by the present method using matrix sizes 1) and 2). The definition of the effective dielectric constant is

$$\epsilon_{\text{eff}} = \left(\frac{\lambda}{\lambda_g}\right)^2 = \left(\frac{\beta}{k_0}\right)^2$$

where λ_g is the guide wavelength. The difference of the zero- and first-order approximation is relatively small. Some test calculations using a larger size matrix have shown that the difference from the first-order solution is so small that the results cannot be distinguished on the graphical figure.

Fig. 3 shows the ratio of guide wavelength to the free-space wavelength. Since the zero- and first-order curves are indistinguishable on this figure, only the first-order results are plotted. The present results are compared with the data in [2], and the agreement is quite good. Experimental results for an open microstrip line reported in [2] are also reproduced.

Typical computation time on the CDC G-20 computer (ten times slower than the IBM 360/75) was about 10–15 s/structure for the first-order approximation when the matrix elements were computed accurately to four digits or better.

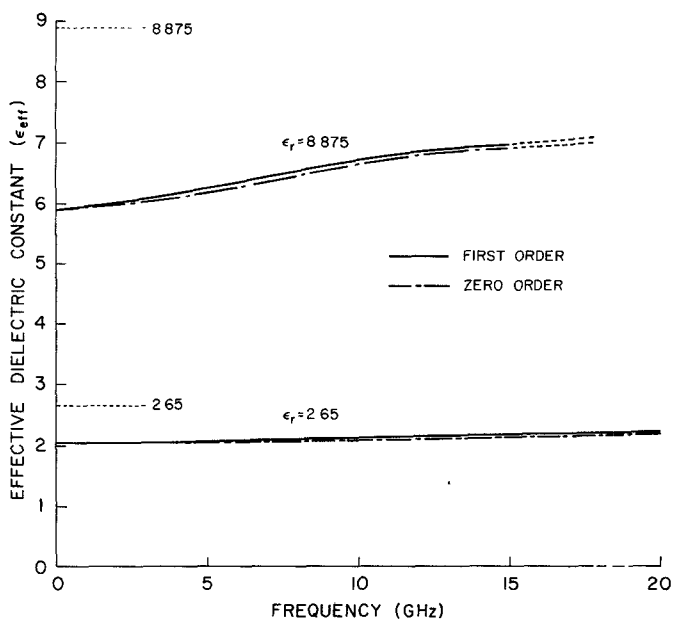

Fig. 2. Effective dielectric constant ϵ_{eff} versus frequency.

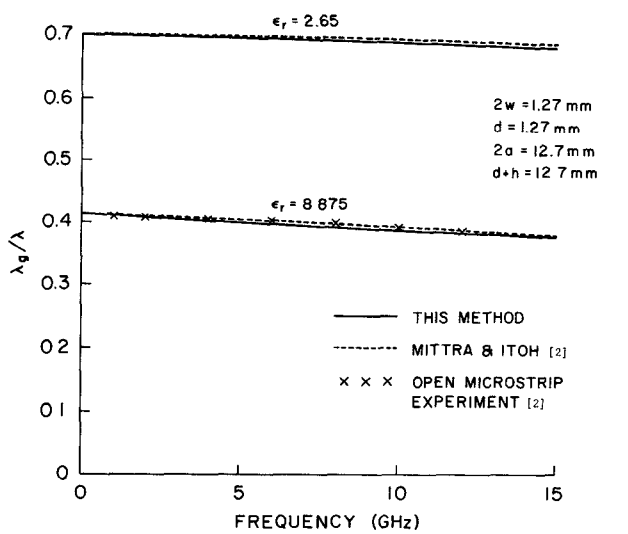

Fig. 3. Normalized guide wavelength λ_g/λ versus frequency.

V. CONCLUSION

An efficient numerical method has been presented for obtaining the dispersion properties of shielded microstrip lines. The method, which is based on Galerkin's method applied in the spectral domain, has a number of numerically attractive features. Numerical results obtained by the present method have been compared with other available data.

REFERENCES

[1] G. I. Zysman and D. Varon, "Wave propagation in microstrip transmission lines," presented at the Int. Microwave Symp., Dallas, Tex., May 1969, Session MAM-I-1.
[2] R. Mittra and T. Itoh, "A new technique for the analysis of the dispersion characteristics of microstrip lines," *IEEE Trans. Microwave Theory Tech.*, vol. MTT-19, pp. 47–56, Jan. 1971.
[3] M. K. Krage and G. I. Haddad, "Frequency-dependent characteristics of microstrip transmission lines," *IEEE Trans. Microwave Theory Tech.*, vol. MTT-20, pp. 678–688, Oct. 1972.
[4] T. Itoh and R. Mittra, "Spectral-domain approach for calculating the dispersion characteristics of microstrip lines," *IEEE Trans. Microwave Theory Tech.* (Short Papers), vol. MTT-21, pp. 496–499, July 1973.
[5] E. J. Denlinger, "A frequency dependent solution for microstrip transmission lines," *IEEE Trans. Microwave Theory Tech.*, vol. MTT-19, pp. 30–39, Jan. 1971.

Mixed Mode Filters

DAVID A. TAGGART AND ROBERT D. WANSELOW,
SENIOR MEMBER, IEEE

***Abstract*—Mixed mode bandpass filters are described which utilize alternating $TE_{011}°$ and $TE_{n11}°$ circular waveguide cavity modes. This novel filter configuration exhibits both excellent unloaded Q and spurious mode response characteristics. The use of mixed resonant modes makes possible the design of microwave filters for both in-line side wall connected cylindrical resonators as well as folded planar filter configurations, whereby cross-coupling between selected resonators can be realized.**

I. INTRODUCTION

It is well known that the design performance of narrow-band cylindrical $TE_{011}°$ mode resonator filters exhibits a very low insertion loss response by virtue of the relatively high unloaded Q that this mode affords [1]. However, due to the relatively large cavity (diameter) size required to support the $TE_{011}°$ mode, resonators operating in this mode tend to display unwanted spurious passband resonances. As described by Matthaei and Weller [2] these spurious resonances can be removed for all practical purposes via the trapped-mode concept. To a lesser degree these spurious modes may also be suppressed by employing alternate right-angle coupling between adjacent cylindrical cavity walls as indicated by [1, p. 923]. However, even though the unloaded Q of the trapped-mode $TE_{011}°$ circular cavity resonator is somewhat higher than that available from conventional rectangular $TE_{101}□$ mode resonantors, it is still well below that realizable from conventional $TE_{011}°$ mode cavity filters. In fact, the unloaded Q of the trapped-mode $TE_{011}°$ resonator is also less than $TE_{n11}°$ mode resonantors ($n > 1$) [2, p. 583]. An additional technique for the elimination of spurious modes is the utilization of a polyiron mode suppressor on the back side of the end wall tuning plunger [3]. Unfortunately, the unloaded Q of the $TE_{011}°$ mode is reduced [1, p. 934] when employing dissipative material.

Manuscript received March 11, 1974; revised May 9, 1974.
The authors are with the TRW Systems Group, Redondo Beach, Calif. 90278.

Rather than trying to suppress or remove the principal mode resonances adjacent to the $TE_{011}°$ mode, this short paper shows that either of the two closest transverse electric modes, namely, the $TE_{211}°$ and $TE_{311}°$ modes, can be employed together with the $TE_{011}°$ mode to yield a mixed mode filter whereby the spurious mode spectrum response will be automatically suppressed to an acceptable level for most narrow-band filter designs. An alternate ordered set combination of $TE_{011}°$ and $TE_{n11}°$ mode resonators can be utilized to yield a good average unloaded Q together with a spurious spectrum response which is superior to the case where all resonators utilize the conventional $TE_{011}°$ mode.

II. DISCUSSION

The cavity configuration of the mixed mode coupled filter takes advantage of the fact that for in-line or straight-through coupling between adjacent cylindrical cavities the E-field distribution is ideal for side wall iris or slot coupling. Fig. 1(a) denotes coupling between the $TE_{011}°$ and $TE_{211}°$ modes. Similarly, the $TE_{011}°$ and $TE_{311}°$ modes can also be coupled as shown in Fig. 1(b). For each mode the D/L ratio will be different in order that all cavities be resonant at the same center frequency. This can be accomplished by selecting a constant diameter for all cavities and adjusting the length via: 1) an end wall plunger [3, p. 323] for the $TE_{011}°$ modes, or 2) radial circumferential screw tuning in the side walls for tuning the $TE_{n11}°$ modes ($n > 0$) at appropriate angles of maximum field intensity. Thus by employing alternate D/L ratio coupled cavities operating with different $TE_{n11}°$ modes the spurious mode spectrum problem usually attendant in conventional $TE_{011}°$ mode filters is substantially alleviated. Furthermore, since the $TE_{211}°$ and $TE_{311}°$ modes exhibit theoretical unloaded Q factors which vary from 1/2 to 2/3 that of the optimum $TE_{011}°$ mode, depending of course on the D/L ratio chosen, the effective or average theoretical unloaded Q of a mixed mode filter will usually fall between 3/4 and 5/6 that of a filter utilizing the conventional $TE_{011}°$ mode in all cavities. These characteristics will be quantitatively described later in this short paper.

In addition to the in-line adjacent cavity coupled configuration as indicated in Fig. 1(a) and (b), the mixed mode filter possesses the potential for realizing in-phase cross-coupled cavity filters as required in linear phase networks [4]. Fig. 2 denotes, for example, an eight section cross-coupled cavity filter utilizing alternate $TE_{011}°$ and $TE_{211}°$ cylindrical cavity modes. In this folded planar layout configuration cavity pairs +36, +27, and +18 are all in-phase cross-coupled, as denoted by the vector field alignments at the cavity coupling holes. Furthermore, if the ordering of the cavity is judiciously chosen so that alternate consecutive vector field cross-couplings possess a sign change (for example −36, +27, and −18), then a nonminimum-phase optimum-amplitude filter response could be realized [5].

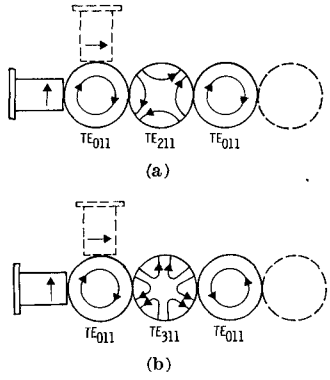

Fig. 1. Electric field distribution of $TE_{n11}°$ modes with $TE_{011}°$ mode. (a) $TE_{211}°$ mixed mode. (b) $TE_{311}°$ mixed mode.

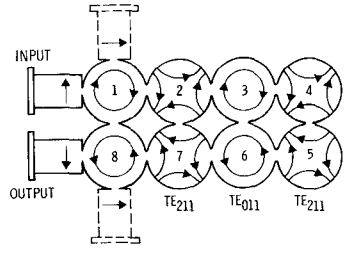

Fig. 2. Low-loss linear phase mixed mode filter configuration.

III. EXPERIMENTAL DATA

A. Single Cavity Resonators

Relative attenuation measurements of in-line (straight-through) versus right-angle coupling of a single cylindrical cavity resonator were made in an effort to compare the transmission characteristics of the $TE_{011}°$ mode with the $TE_{211}°$ and $TE_{311}°$ mode resonances. These data are presented in Table I. Fig. 3(a) defines the coupling geometries. The $TE_{011}°$ mode was tuned with a plunger in one end cavity wall whereas the two $TE_{n11}°$ ($n = 2$ or 3) mode cavities were of a split block configuration (circumferentially split half way between the end walls) and screw tuned.

TABLE I[a]
SINGLE CAVITY PRINCIPAL MODE STUDY

PRIMARY CAVITY MODE	FILTER COUPLING CONFIGURATION	APERTURE COUPLING IRIS	FREQUENCY (MHZ)	ATTENUATION LEVEL (db)		
				TE_{011}	TE_{211}	TE_{311}
TE_{011}	In-Line	Slot	7507	2.5		
			6616		5.1	
			7928			3.5
TE_{011}	Rt. Angle	Slot	7507	1.9		
			6616		5.1	
			7966			20.0
TE_{211}	In-Line	Slot	7512		0.85	
			8335	1.05		
			8671			0.3
TE_{211}	Rt. Angle	Slot	7512		0.85	
			8335	1.05		
			8751			26.5
TE_{311}	In-Line	Slot	7658			0.95
			6296		4.1	
			7258	2.8		
TE_{311}	Rt. Angle	Slot	7705			22.5
			6296		4.1	
			7258	2.7		

[a] All mode resonances not listed in Tables I–III were greater than 60 dB below the 0-dB attenuation reference level.

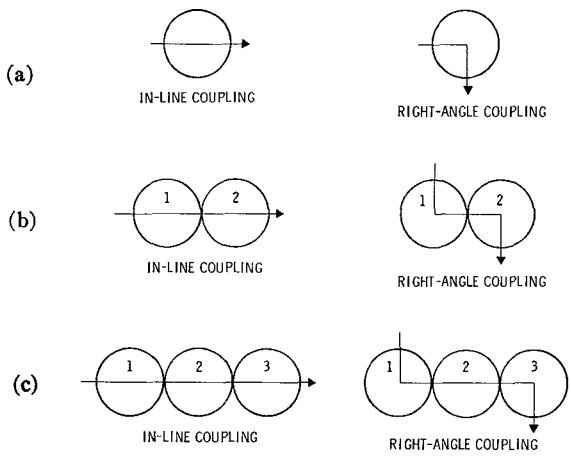

Fig. 3. Experimental coupling configurations studied. (a) Single cavity resonators. (b) Two cavity configurations. (c) Three cavity configurations.

TABLE II
TWO CAVITY MODE STUDY

CAVITY MODE							ATTENUATION LEVEL (db)		
INPUT CAVITY NO. 1	OUTPUT CAVITY NO. 2	FILTER COUPLING CONFIGURATION	CENTER APERTURE COUPLING IRIS	THEORETICAL AVERAGE QU	MEASURED AVERAGE QU	FREQUENCY (MHZ)	TE_{011}	TE_{211}	TE_{311}
TE_{011}	TE_{011}	In-Line	Circle	30368	20303	7450	0.31		
						6504		0.8	
						7870			0.25
TE_{011}	TE_{011}	Rt. Angle	Circle	30368	20293	7450	0.35		
						6533		3.5	
						7928			7.0
TE_{011}	TE_{011}	Rt. Angle	Slot	30368	20293	7450	0.35		
						6533		3.5	
						7928			24.0
TE_{211}	TE_{011}	In-Line	Circle	23021	12923	7450	0.55		
						6458		21.0[a]	
						8292			17.0
TE_{311}	TE_{011}	In-Line	Circle	24497	13703	7450	0.47		
						---		>40.0	
						7867			30.0[a]

[a] This spur is a second cavity resonance as seen at the output.

In-line and right-angle coupling yield essentially the same attenuation level for either the $TE_{011}°$ or the $TE_{211}°$ modes because of their quadrature E-field symmetry. Furthermore, as expected, the right-angle coupling of the $TE_{311}°$ mode is reduced by the order of 20 dB. The measured data exhibit a slightly closer frequency mode spectrum relative to the $TE_{011}°$ resonance than theory indicates. This is due in part to the relative coupling hole size or variable external coupling for each mode and scales very closely with the published data by Montgomery [3, p. 324]. Thus this summary is useful as a base for comparing the relative reduction of adjacent modes as well as denoting the measured spectrum location of these modes for both the two and three cavity mixed mode filter studies.

B. Two Cavity Filters

Tests were conducted on several two cavity mixed mode filter configurations to determine the relative spurious spectrum response as well as the average unloaded Q obtainable. All filters tuned to 7450 MHz were 0.01-dB passband ripple Chebyshev designs of less than 0.1-percent bandwidth fabricated out of copper. The in-line and right-angle coupled filter layouts are denoted in Fig. 3(b). The results of transmission tests for these configurations are shown in Table II.

In all cases the average measured unloaded Q was more than 55 percent that of the theoretical average. However, both the measured and theoretical values could be improved by at least 10 percent if the D/L ratio of the $TE_{011}°$ mode cavities was chosen closer to the optimum region of 1.0 but at the expense of a slight degradation in passband insertion loss slope which becomes more pronounced as a filter design is required to operate closer to cutoff. For these tests the D/L ratio was about 1.93 for the $TE_{011}°$ cavities and approximately 2.40 and 1.74 for the $TE_{211}°$ and $TE_{311}°$ resonators, respectively, where all cavities were constructed with the same diameter, namely, 2.430 in.

It is of interest to note that the adjacent spur level for the $TE_{211}°$—$TE_{011}°$ and $TE_{311}°$—$TE_{011}°$ in-line coupled cavity configuration is considerably reduced below that of the reference $TE_{011}°$—$TE_{011}°$ in-line coupled cavity case. Furthermore, in the case of right-angle coupling between $TE_{011}°$—$TE_{011}°$ cavities note the improvement in the reduction of the $TE_{311}°$ mode spur when slot coupling

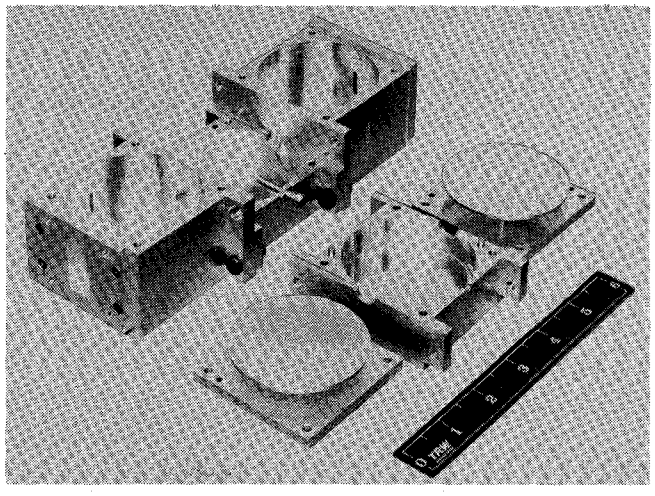

Fig. 4. Experimental three cavity filter.

TABLE III
THREE CAVITY MODE STUDY

CAVITY MODE								ATTENUATION LEVEL (db)		
INPUT CAVITY NO. 1	CENTER CAVITY NO. 2	OUTPUT CAVITY NO. 3	FILTER COUPLING CONFIGURATION	CENTER CAVITY COUPLING IRIS	THEORETICAL AVERAGE QU	MEASURED AVERAGE QU	FREQUENCY (MHZ)	TE_{011}	TE_{211}	TE_{311}
TE_{011}	TE_{011}	TE_{011}	In-Line	Circle	30059	21298	7518	0.56		
							6618		0.70	
							7933			0.50
TE_{011}	TE_{011}	TE_{011}	Rt. Angle	Circle	30057	19530	7519	0.60		
							6624		4.0	
							8047			10.5
TE_{011}	TE_{211}	TE_{011}	In-Line	Circle	25228	15810	7518	0.69		
							6537		28.0	
							7978			>40.0
TE_{011}	TE_{311}	TE_{011}	In-Line	Circle	26213	18530	7517	0.65		
							6562		36.0	
							7910			37.0

is employed between the two cavities rather than the circular hole iris. Table II data indicate that either the $TE_{211}°$ or $TE_{311}°$ mode is acceptable for in-line mixed mode filter design as will be further demonstrated in the next section.

C. Three Cavity Filters

Fig. 3(c) shows the two coupling configurations employed for testing the experimental three section copper filter illustrated in the exploded photo of Fig. 4. The input and output cavities were designed to be resonant in the $TE_{011}°$ mode and were tuned with identical flat cylindrical plate plungers. The external input and output cavity coupling obstacles were linear slots. The internal cavity was fabricated in a split block type construction to yield a high unloaded Q for all the various modes tested. A tuning screw is shown for frequency adjustment of the $TE_{211}°$ mode of operation. As before with the two section filters, the three section units were 0.01-dB Chebyshev design centered at about 7518 MHz.

Table III itemizes the results of the filter characteristics. It should be noted that the right-angle cavity coupling test with all cavities operating in the $TE_{011}°$ mode yields a spur spectrum which agrees very closely with that published in [1, p. 922] and which is considerably better than the in-line configuration, as anticipated. For the two mixed mode filters tested the $TE_{211}°$ and $TE_{311}°$ spurs are reduced to a level of 28 dB or better. This spur rejection will increase as the number of filter cavities is increased. For comparison, Table II indicates that the two section mixed mode filters exhibit an adjacent spur spectrum of 17 dB or better. Furthermore, with reference to the single $TE_{011}°$ mode cavity (Table I) the relative attenuation level of in-line coupled $TE_{211}°$ and $TE_{311}°$ spur modes was less than 3 dB. Therefore, the staggering of circular cavity modes by employing a mixed mode filter is useful for the reduction of undesired spurious modes.

It is not the intent of the mixed mode filter concept to suppress all spurious modes over an extremely broad spectrum; however, the technique accomplishes adequate rejection over at least a 50-percent bandwidth, i.e., from the $TE_{211}°$ mode spur out to at least the region of a closely spaced double mode resonance which probably is the $TE_{411}°$ and $TE_{121}°$ higher order modes. This double mode resonance was also displayed in [1, p. 922, fig. 15.04.1]. The spur level rejection beyond the $TE_{311}°$ mode resonance out to 10 GHz is considerably improved when employing mixed mode coupling.

IV. CONCLUSIONS

The use of mixed resonant cavity circular waveguide modes to realize microwave bandpass filters was demonstrated for obtaining a prescribed low-loss passband with excellent stopbands over at least a 50-percent bandwidth. Thus narrow-band communication filter designs could be enhanced over conventional $TE_{101}□$ rectangu-

lar or TE_{111}° circular waveguide networks through the application of the mixed mode filter. A novel feature of this concept is its potential capability of realizing planar cross-coupled filter designs.

REFERENCES

[1] G. L. Matthaei, L. Young, and E. M. T. Jones, *Microwave Filters, Impedance-Matching Networks, and Coupling Structures*. New York: McGraw-Hill, pp. 921–934.

[2] G. L. Matthaei and D. B. Weller, "Circular TE_{011}-mode, trapped-mode band-pass filters," *IEEE Trans. Microwave Theory Tech. (Special Issue on Microwave Filters)*, vol. MTT-13, pp. 581–589, Sept. 1965.

[3] C. G. Montgomery, *Techniques of Microwave Measurement* (Radiation Laboratories Series, vol. 11). New York: McGraw-Hill, 1947, pp. 323–324.

[4] J. D. Rhodes, "The generalized direct-coupled cavity linear phase filter," *IEEE Trans. Microwave Theory Tech.*, vol. MTT-18, pp. 308–313, June 1970.

[5] A. E. Atia and A. E. Williams, "Nonminimum-phase optimum-amplitude bandpass waveguide filters," *IEEE Trans. Microwave Theory Tech.*, vol. MTT-22, pp. 425–431, Apr. 1974.

Letters

The Admittance Matrix of Coupled Transmission Lines

A. I. GRAYZEL

***Abstract*—An alternate derivation of the admittance matrix of n coupled lines is presented. The method uses the superposition of two modes of excitation analagous to the even and odd mode excitation used for the analysis of two coupled lines. Only mutual capacitance to adjacent lines is considered.**

In this letter an alternate derivation of the admittance matrix derived by Riblet [1] is presented. The configuration is shown in Fig. 1 and the matrix is defined by (1) which are identical to [1, fig. 1 and eq. (1)]:

$$\begin{vmatrix} I_{1a} \\ I_{1b} \\ I_{2a} \\ I_{2b} \\ I_{3a} \\ I_{3b} \\ \vdots \\ I_{na} \\ I_{nb} \end{vmatrix} = p \begin{vmatrix} Y_{11} & -Y_{11}t & Y_{12} & -Y_{12}t & 0 & \cdot & \cdot & & & & \\ -Y_{11}t & Y_{11} & -Y_{12}t & Y_{12} & 0 & \cdot & \cdot & & & & \\ Y_{12} & -Y_{12}t & Y_{22} & -Y_{22}t & Y_{23} & -Y_{23}t & 0 & \cdot & \cdot & & \\ -Y_{12}t & Y_{12} & -Y_{22}t & Y_{22} & -Y_{23}t & Y_{23} & 0 & \cdot & \cdot & & \\ 0 & 0 & Y_{23} & -Y_{23}t & Y_{33} & -Y_{33}t & Y_{34} & -Y_{34}t & 0 & \cdot & \cdot \\ \cdot & \cdot & -Y_{23}t & Y_{23} & -Y_{32}t & Y_{33} & -Y_{34}t & Y_{34} & 0 & \cdot & \cdot \\ & & & & & & & & & & \\ \cdot & \cdot & \cdot & \cdot & \cdot & \cdot & \cdot & \cdot & Y_{nn} & \cdot & -Y_{nn}t \\ \cdot & \cdot & \cdot & \cdot & \cdot & \cdot & \cdot & \cdot & -Y_{nn}t & \cdot & Y_{nn} \end{vmatrix} \cdot \begin{vmatrix} V_{1a} \\ V_{1b} \\ V_{2a} \\ V_{2b} \\ V_{3a} \\ V_{3b} \\ \vdots \\ V_{na} \\ V_{nb} \end{vmatrix} \tag{1}$$

where $p = -j \cot(\theta)$ and $t = \sec(\theta)$.

From the definition of the admittance matrix

$$y_{i,j}^{u,v} = \left.\frac{I_{j,v}}{V_{i,u}}\right| \text{ all voltages are zero except } V_{i,u} \tag{2}$$

where $I_{j,v}$ is the current flowing into the jv node and $V_{i,u}$ is the voltage of node iu with respect to the ground plane. i and j take on values from 1 through n, u and v are either a or b. Reciprocity requires that $y_{i,j}^{u,v} = y_{j,i}^{v,u}$ and hence we can find all of the element values of the admittance matrix as given in (2) by connecting a voltage source to only one side of each line, i.e., to nodes ia as shown in Fig. 2. Symmetry requires that $y_{i,j}^{u,v} = y_{i,j}^{v,u}$ and $y_{i,j}^{u,u} = y_{i,j}^{v,v}$.

We will solve the problem of Fig. 2 by superposition of the circuit of Fig. 3(a) and the circuit of Fig. 3(b). We will refer to the excitation of Fig. 3(a) as mode 1 excitation and that of Fig. 3(b) as mode 2 excitation. Under mode 1 excitation the incident voltage wave on all of the lines will be equal. Since all of the lines are terminated in a short circuit the reflected waves will also be equal. Thus the voltage on all of the lines will be equal for their entire length. It is well known that for a wave propagating in the TEM mode the fields in the transverse plane satisfy Laplace's equation, and hence the characteristic impedances can be determined from a static field configuration or from the static capacitances. In Fig. 4(a) the static capacitances of the coupled lines are shown. For the mode 1 excitation the voltage on all of the lines are equal and hence there can be no current through the mutual capacitances. We can treat the lines as uncoupled lines with capacitance to ground per unit length equal to C_i. Under mode 2 excitation the incident voltage on line i will be the negative of the voltage on all of the other lines. Since all of the lines have short-circuited terminations the reflected voltage wave

Manuscript received October 10, 1973; revised June 5, 1974.
The author is at 29 Forest Street, Somerville, Mass. 02143.